Flip-Chip Assembly Development via Modified Reflowable Underfill Process

Ping Miao, Yixin Chew, Tie Wang and Louis Foo

Questech Solutions Pte Ltd, Singapore
33 Marsiling Industrial Estate, Road 3, #03-01, Singapore 739256
e-mail: pmiao@qts-aps.com.sg
Tel: (65)-3684822, Fax: (65)-3685277

Abstract

This paper presents two flip-chip assembly processes that enable an underfill with higher filler loading to be incorporated into the package. The first process includes dispensing the underfill containing higher filler loading on substrate surface, followed by chip placement and solder reflow under thermal compression. Apart from this, the second approach is virtually the modification of standard reflowable underfill process. The underfill with higher filler loading was spin-coated onto a bumped wafer surface and then cured. Subsequently, the top portion of bumps was exposed by laser treatment prior to wafer dicing. The diced chips with low CTE coating on surface already were assembled via standard reflowable underfill process that includes dispensing reflowable underfill, chip placement and solder reflow through reflow oven.

I. Introduction

Flip-chip technology on an organic substrate has been used in vast applications in the microelectronic industry. When assembled on the organic substrate, the large CTE mismatch between the die and substrate necessitates the use of underfill materials to enhance the thermo-mechanical reliability of the interconnections [1]. Currently, underfilling is carried out by the conventional capillary flow process and reflowable underfill process (no-flow underfill process). With the increase in die size, I/O numbers, and decrease of bump pitch, the capillary flow method has become increasing difficult and time consuming. However, the reflowable underfill process provides the solutions through compression flow of underfill that significantly reduces underfill flow time [2,3]. In addition to the high throughput, this process also has less process complexity and capital equipment requirements by eliminating some assembly steps. Unfortunately, using solid filler to reduce the CTE of underfill, has become a limitation of this process. The filler particles are easily trapped between the solder bump and bump pads, hence preventing the formation of solder joints. Because of this, the reflowable underfill has lower filler loading or no filler at all and therefore CTE of this material turns out to be around 70~90 ppm/^{o}C that is higher than commonly expected value. Currently, the main technical challenge lies in how to reduce CTE mismatch in flip-chip assembly, in particular for packages having larger die.

This paper describes two reflowable underfill processes that enable underfill with higher filler loading to be incorporated into the package, namely thermo-compression reflowable (TCR) process and wafer-level coating (WLC) process. In order to prepare proper underfill for these two processes, DOE (Design of Experiments) was used to discover what factors affect the properties of reflowable underfill.

II. Formulations and testing procedures

Three different formulations were evaluated during the course of this work. Underfill I (UI) was formulated for thermo-compression reflowable process studies while Underfill II (UII) and underfill III (UIII) was for wafer-coating studies. All formulations were epoxy resin/ anhydride based although the cure chemistry and resin functionality were varied to give different final material properties. Metal acetylacetonate was used as curing catalyst for UI and UIII while imidazole compound was used to catalyze the curing reaction of UII. UI and UII were filled with spherical silica filler at 55% weight loading. The underfill samples were produced by dispersing the silica particles in epoxy matrix using a special disperser.

DSC studies were carried out via a modulated DSC (TA Instruments, Model 2920). About 10 mg sample in hermetic DSC sample pan was heated in the DSC cell at 10°C /min to 300°C. CTE and Tg were measured on a Thermomechanical Analyzer (TA Instruments, Model 2940). The specimen was prepared by fully curing the sample at 150°C for 1.5 hour. After curing, the sample was ground to a round tablet with a diameter of 5 mm and thickness of 4-5 mm and heated in the TMA instruments from room temperature to 200 °C at a rate of 10°C/min. The viscosity was measured by a Programmable Rheometer (Brookfield, Model DV-111) at room temperature (25°C). A Dage 2400 shear tool is utilized to perform die shear.

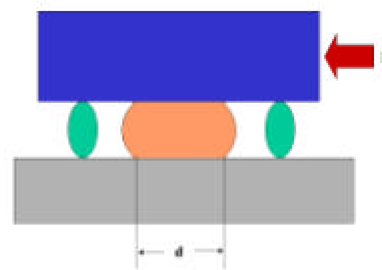

Fig. 1 Schematic of shear testing

The adhesion of underfill to SiN passivation (U/SiN) and solder mask (PSR 4000-AUS303, U/SM) has been tested as the response for DOE experiments. A small drop of underfill was placed in the center of testing tools (Figure 1) and the sample was cured at 150 °C for 1.5 hours.

$$\text{Shear Strength (S, PSI)} = \text{Force (Kg)} / \text{Area (mm}^2)$$
$$S = 4F / \pi d^2$$

6-inch silicon wafer bumped with eutectic (63: 37 Sn/Pb) solder was used in this TCR and WLC process study. Table 1 lists the specification of test wafer and die.

Table 1. Specification of test vehicle

Wafer size	6'
Chip number	140
Chip size	10.30 × 10.30mm
Configuration	Full array
I/O	1600
Pitch	250 µm
Bump height	100 µm
Substrate	BT laminate
Surface finish	Ni/Au
Solder mask opening	170 µm
S/M thickness	40 µm

III. Process Description

IIIa. Thermo-compression reflow process

In TCR process, the underfill with high silica loading was dispensed on the surface of organic substrate. In order to eliminate the voids and reduce the viscosity of underfill materials, the substrate was pre-heated to ~ 90 °C. The die was picked and placed onto the substrate and held at high temperature under certain force for 20 seconds to allow the formation of solder joints. Finally, the assembly units were sent to cure at 150°C for 1.5 h.

The yield of this TCR process is strongly dependable on the properties of underfill that will be discussed later in this paper. In addition to the underfill properties, the force and temperature as well as their ramping rate also play key roles in this study. Using the normal oven reflow process, whereby no holding force is applied during solder reflow, less than 10% of solder bump were found to form the solder joints even when the silica loading of underfill is only 25 wt %. Most solder bumps did not make contact with Ni/Au pad and there was underfill material trapped between the solder and pad. When the force was increased to 50 N, more than 99% solders reflowed to form good solder joints. These few failed joints are due to the trapping of silica fillers between the bump and bump pad. On the other hand, when the force increased to 100 N, all solders reflowed and no dry joints were found after cross-section analysis. The average standoff of solder joints is 60 µm. After optimizing the process, the holding force of 75 N was used to assemble 20 units for reliability test.

In order to eliminate the trapping of silica particles inside solder joints (Figure 3), the bonding force can not be too high before and during solder melting. Thus the force and temperature ramping must be carefully controlled. In addition, fast ramping of temperature will generate plenty of voids. High reflow temperature is beneficial for solder reflow. However, this will result in serious outgassing from underfill.

Figure 4 illustrates the optimized force and temperature program that is used for TCR process. Initial bonding head temperature and placing force were set at 150°C and 20N respectively. Then it took 10s to ramp to 230°C and 75N. The whole assembly was subsequently kept for another 15s to reflow bumps. This bonding program leads to a package with good solder joint and acceptable void level (Figure 5).

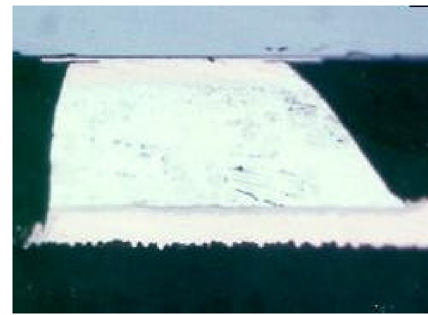

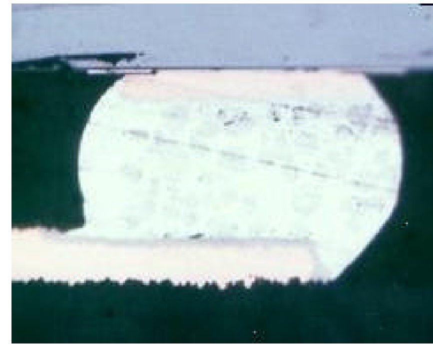

Figure 2. The solder joints of TCR process, F=75N

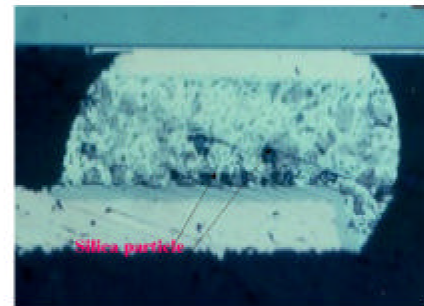

Fig. 3 The silica was trapped inside the solder bump when the force and temperature was too high during solder melting.

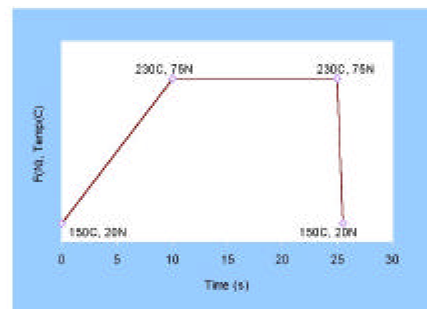

Fig. 4 The ramping profile of temperature and force

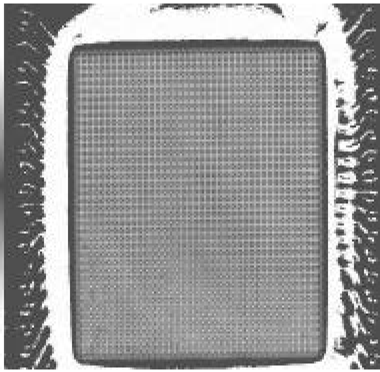

Fig. 5 C-Sam image of TCR package

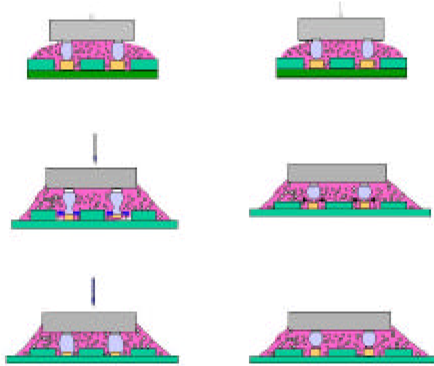

Fig. 6 Schematics of TCR process with (left) and without (right) applying holding force.

The schematic diagram of thermo-compression reflowable process is shown in Figure 6. In the first step, the solder bump contacted with Ni/Au pad at a point. This contact point is critical for the following solder wetting process. When the solder melted, it starts to wet the Ni/Au surface from the contact point. The underfill was pushed away from the surface of Ni/Au by the "wetting force" of melten solder. To keep the contact point for wetting, certain level force is required during reflow process. Otherwise, the underfill flowing at elevated temperature could result in a gap between the solder and pad, which prevented the formation of solder joints. In addition, the contact point must be formed before the solder melt. Otherwise, the filler particles could be easily trapped inside the solder joints.

IIIb. Wafer-level coating process

Figure 7 shows the WLC process. First, the underfill (UII) was spin-coated onto the surface of wafer (Figure 7a) and cured at 125°C for 20 minutes. Second, the top layer of coating material was removed by laser etching (Figure 7b). The wafer was then singulated (Figure 7c). The single chip was assembled on an organic substrate using common reflowable underfill process, i.e. dispensing second layer of underfill (UIII) onto the substrate, picking and placing the coated chips onto the substrate (Figure 7d), reflowing the units in reflow oven and fully curing materials. (Figure 7e). This process provides another way to introduce silica filler into reflowable underfill process without using high force and sacrificing the throughput.

The underfill for coating studies was a solvent-free, silica filler loaded material. The quality of coating film was dependent strongly on film formability of underfill. Thus, a surfactant was used to improve the surface tension of coating material. This surfactant can enhance the wetting of underfill to wafer surface and prevent underfill contract from silicone surface during thermo-curing of underfill.

Coating can be done by screen printing, spin coating or extrusion approaches. In this study, a spin- coat machine was used. According to the packaging structure (Fig. 7), the coating thickness (after fully curing) should be controlled to ~ 60% of bump height. Thus, the spin-coating program can be optimized according to the viscosity of material and the coating thickness.

Figure 8 shows the cross-section image of one bump from coated wafer. The thickness of coating in the area between bumps (H) were around 60 µm. The underfill was thicker around the bump and there was a thin layer of underfill covering the top of the bump (Figure 9). This layer will hinder the formation of solder joints.

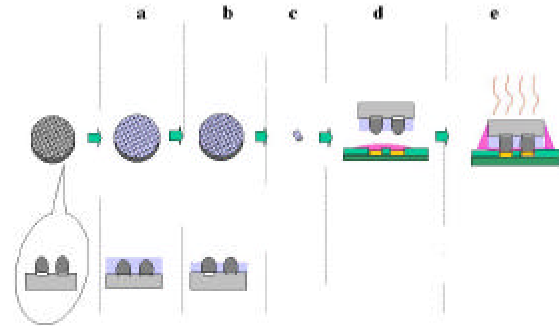

Fig. 7 Schematic diagram of WLC process

Fig. 8 Cross-section image of a coated wafer bump before and after laser etching

Several methods can be used to remove this layer of underfill, such as a B-stage approach [4], mechanical cutting [5] and laser or plasma etching. This paper describes the laser etching method that can remove the upper layer underfill efficiently. A KrF excimer laser with wavelength of 248 nm was used as a light source and 400-600 mJ/cm^2 was applied to etch out fully cured epoxy resin. The etched residue was sucked up by a vacuum system. Figure 10 shows coated wafer surface before and after etching. After etching, the bump was exposed and the surface was free

from underfill and silica particles. The surface of the underfill became rougher after etching. This rough surface enhances the adhesion of second layer underfill to first layer underfill. It is interesting to find that the material surrounding the bump is easier to be etched out than other part. Thus, the thickness of coated material between bumps is not significantly affected (Figure 8).

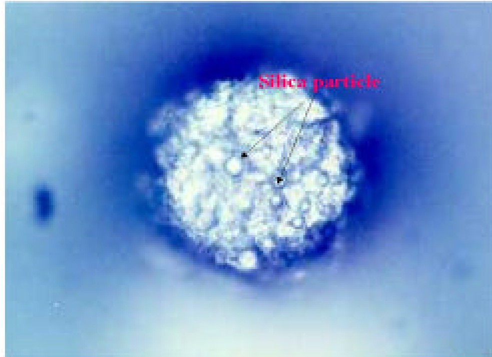

Fig. 9 The top layer of bump before etching. This top part of bump has been flattened by pressing the bump.

In order to form the solder joints, a second layer material (UIII) which was free from solid filler was used via common reflowable process. The solder joints are shown in Figure 11 and 12. The shape of the solder joints is dependent on the exposed height of bump that is, in turn, determined by the coating thickness and etching degree. Figure 11 shows the solder joints that are formed from less etched chips while Figure 12 was the joint from heavy etched chips. The joint of Figure 11 looks like "vase" with a "wrest" with a standoff of 75 µm which was higher than that of Figure 12. Figure 13 exhibits a two-layer underfill structure of a packaging. The layer on chip side is a high silica loading underfill (UII) while the very thin layer on substrate side is a solid filler free material (UIII). By using this method, sufficient fillet is obtained which, in some degree, ensure the good reliability. C-SAM image (Figure 14) shows that the number and size of voids are acceptable.

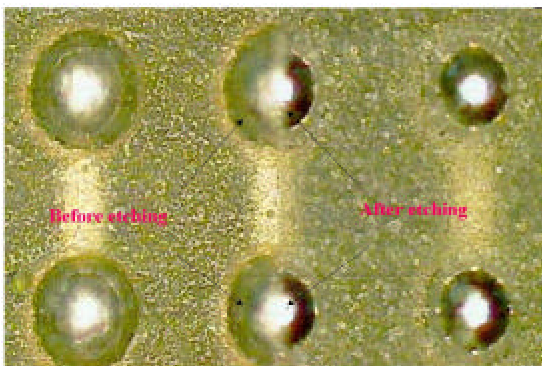

Fig. 10 The surface of a bump before and after etching.

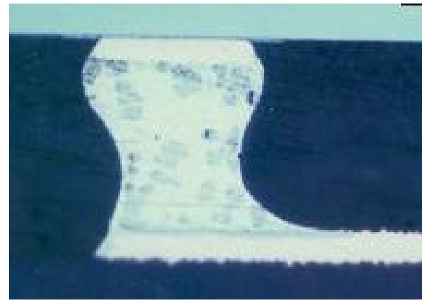

Fig. 11 The Solder joint of WLC process.

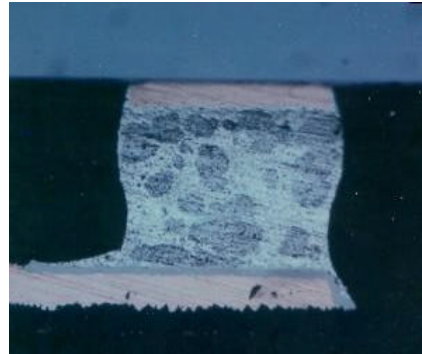

Fig. 12 Solder joint of WLC process.

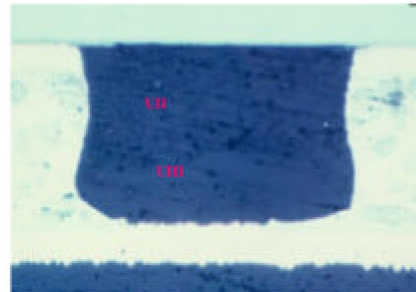

Fig 13. The two-layer structure of WLC packaging

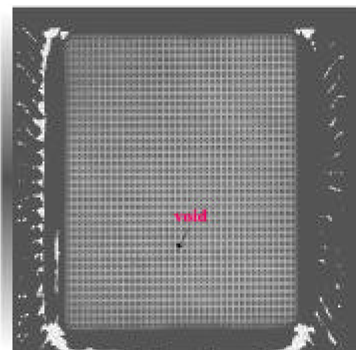

Fig. 14. C-SAM image of WLC packaging

IV. Reflowable underfills

The key of the reflowable underfill process is the selection of underfill materials. Underfill for this study

should have proper curing properties, strong adhesion to chip passivation and solder mask of substrate, proper rheology for processing, low CTE to match the components and reasonable modules and glass translation temperature. Figure 15 shows the DSC analysis of UI, UII and UIII. The curing profiles of UI and UIII must match the solder reflow profile, as such, UI and UIII should not gel before solder bump reflow. These two materials have sufficient fluxing ability to remove the oxide of eutectic solders. UII, which was formulated for spin coating, was a fast cure material without self-fluxing capability.

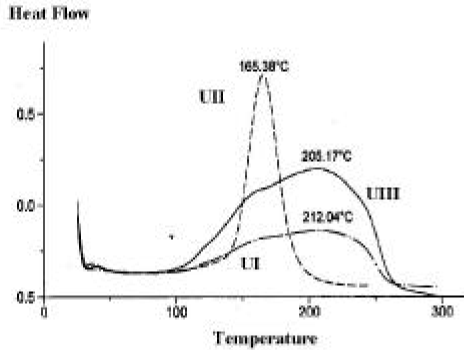

Fig. 15 Curing profile of underfillUI, UII and UIII.

CTE mismatch is a great concern in this study. Figure 16 exhibits the TMA results of theses three materials. The silica loading of UI and UII was in the range of 50-55%. The CTE (α_1) of these two materials were around 40 ppm/°C. CTE of epoxy type underfill depended on the silica loading, filler size and the additives of the formulation. When the silica loading reaches 50%, there is a great reduction of CTE. Thus, normally, the silica loading was above 55%. The size of silica particles also affect the CTE of materials. At same loading level, the smaller size silica resulted in lower CTE. For example, at 55% loading, 5 µm silica loaded underfill has CTE of 33 ppm/°C while 10 µm silica loaded underfill has CTE of 37 ppm/°C. In addition, the additives also play a role in CTE issue. Those elastomer additives may increase the CTE and reduce the Tg of underfills.

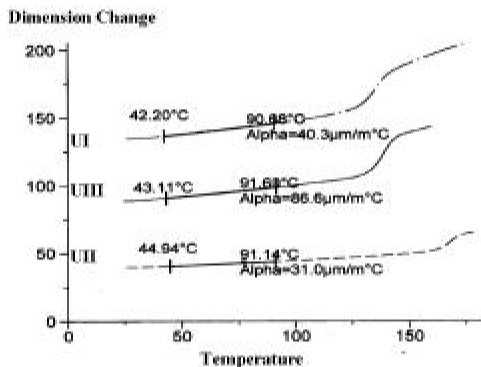

Fig. 16 CTE and Tg of underfill UI, UII and UIII

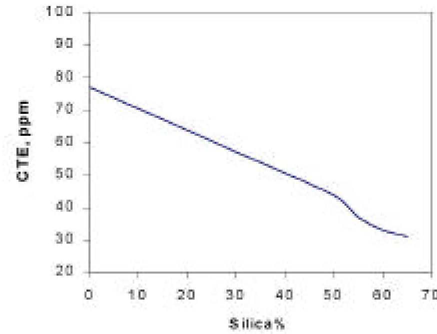

Fig.17. Effect of Silica loading on CTE

Another important property of underfill is its adhesive strength on the surface of other package components. Poor adhesion of die passivation/underfill and underfill/solder mask will resulted in the delamination of the interface and therefore poor reliability of package. Many factors affect the adhesion strength of materials [6], including the underfill formulation, passivation and solder mask types, roughness of these surface as well as the type of additives and fillers in underfill. As discussed above, several additives were added to improve the properties of underfills, including silica particles, wetting enhancing agent, coupling agent and fluxing agent, etc. Some additives can enhance the adhesion while others have negative effects on adhesion. A set of DOE experiments was designed to study the effects of those additives. Table 2 lists the experiments of DOE. Wetting agent (siloxane), silica, and coupling agent (silane) were selected as the main factors and the shear strength (Shear 1: U/SiN, Shear 2: U/SM)) was used to measure the adhesion of materials. (response of DOE)

Table 2. DOE experiments

	Silica (%)	Siloxane (phr)	Silane (phr)	Shear1 (psi)	Shear2 (psi)
1	25	0.25	1.0	8600	5560
2	25	0.25	1.75	7020	4150
3	25	1.0	1.0	7850	3960
4	25	1.0	1.75	6970	5960
5	55	0.25	1.0	6450	3560
6	55	0.25	1.75	6640	3100
7	55	1.0	1.0	4490	3230
8	55	1.0	1.75	5060	3130

The results of DOE experiments are shown in Table 3 and Figure 18–20. In the case of die passivation, the significant effects are the loading amount of silica and siloxane. Among them, silica loading is the most significant factor influencing adhesion strength. High silica loading will significantly reduce the shear strength due to the reduction of the resin amount in underfill system. The more significant factor is siloxane which also has a negative effect on the adhesion strength. Silane is the least significant. Increasing the silane amount did not significantly increasing the adhesion. In contrast, too much of silane may reduce the adhesion slightly. The Coefficient of Determination (r^2) of

shear 1 is ~ 99%, indicating that the model as fitted explains 99% of the variability in shear 1.

Table 3. Estimated effects for shear 1 and shear 2

Factors	Shear 1	Shear 2
A. silica	-1995.0	-1650.0
B. siloxane	-1085.0	-25.0
C. silane	-435.0	5.0
AB	-680.0	-125.0
AC	810.0	-285.0
BC	270.0	940.0
r^2	99.9119	86.5085

Table 2 also indicates that the adhesion of underfill to solder mask is much weaker than that of SiN passivation. As in the case of the passivation, the silica loading has the main effect and the silane has the least effect on the adhesion strength of U/SM (Figure 20). However, unlike the case of U/SiN, siloxane did not result in a significant change in U/SM.

Based on the above results of DOE, the conclusions on the adhesion strength of silica filled underfill are as follow.

1. The adhesion strength is reduced by loading silica fillers. For 55% loading of silica, the die shear strength is only about half of that of the non-filled underfill.
2. Adhesion on SiN is stronger than the adhesion on solder mask. Thus, future works should be focused more on the underfill/SM interface.
3. Addition of wetting agents can significantly reduce the adhesion of underfill/SiN, but have small effect on the adhesion of underfill/SM. A more effective wetting agent is needed to reduce the amount of siloxane in formulations.
4. More coupling agent (silane compounds) is not useful for the adhesion of underfill/SM and underfill/SiN. In contrast, it may produce out-gassing problem due to its relatively low boiling point.

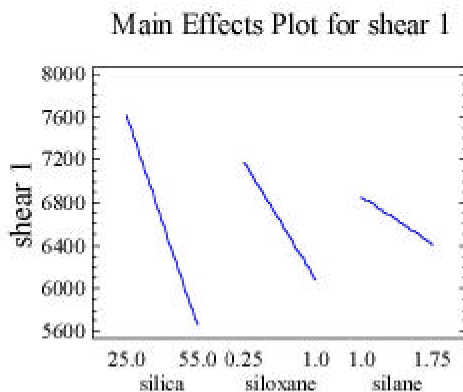

Fig. 18 The effects of silica, silane and siloxane on the adhesion of U/SiN.

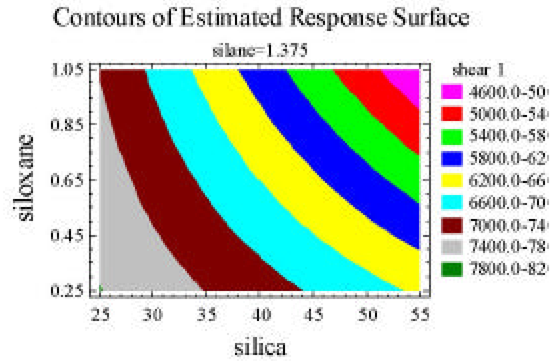

Fig. 19 The response plots of main effects (silica and siloxane) on the adhesion of U/SiN

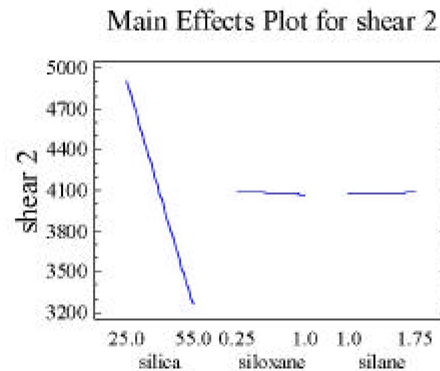

Fig. 20 The effects of silica, silane and siloxane on the adhesion of U/SM

V. Conclusions

Two reflowable processes were proposed to apply the low CTE underfill. By thermo-compression reflow process, the silica was introduced into the package directly. After process optimization, solder joints, which are free of trapped fillers between bump and pad are obtained by applying underfill which has filler loading up to 55%. Alternatively, the low CTE underfills can also be applied by wafer coating-etching approach. For this reflowable underfill process, two-layer structure was clearly demonstrated with one thick layer of low CTE underfill at the chip side and another thin layer of high CTE reflowable underfill at the substrate side. The keys to achieving high packaging yield and better reliability is to making underfill which has low CTE, yet with strong adhesion, sufficient fluxing ability. Studies of package reliability, evaluation of other coating and etching methods are in process.

Acknowledgement

Finally, we are deeply grateful to Dr Lu Yongfeng and Dr Ren Zhongmin in Data Storage Institute, Singapore who have been so helpful in conducting the laser etching experiment.

References

1. D. Suryanarayana and D. S. Farquhar, "Underfill encapsulant for flip chip applications" in *Chip on Board*, J H. Lau, Ed. New York:Van Nostrand Reinhold, p. 504, 1994
2. C. P. Wong, D. F. Baldwin, M. B. Vincent, B. Fennel, L. J. Wang, and S. H. Shi, "Characterization of a no-flow underfill encapsulent during the solder reflow process," in *Proceedings of the 48th Electronic Components and Technology Conference '98*, p.1253, 1998
3. N. W Pascarella and D. F. Baldwin, "Compression flow modeling encapsulants for low cost flip-chip assembly," *IEEE Transactions on Components, Packaging, and Manufacturing Technology-Part C*, Vol. 21 (4), p. 325, 1998
4. S. H. Shi, T. Yamashita, and C. P. Wong, "Development of the wafer level compressive-flow underfill process and its involved materials," *IEEE Transactions on Electronics Packaging Manufacturing*, 22(4), p.274, 1999
5. M. Topper, J. auersperg, V. Glaw, K. Kaskoun, E. Prrack, B. Keser, P. Coskina, D. Jager, D. petter, O. Ehrmann, K. Samulewicz, C. Meinherz, S. Fehlberg, C. Karduck, H. Reichl, "Fab Integrated Packaging (FIP): A new concept for high reliability wafer level chip size packaging," in *Proceedings of the 48th Electronic Components and Technology Conference '2000*, p. 74, 2000
6. Q. Yao, J. M. Qu, J. L. Wu and C. P. Wong, "Characterization of underfill/substrate interfacial toughhness enhancement by silane additives," *IEEE Transactions on Components, Packaging, and Manufacturing Technology-Part C*, Vol. 22 (4), p. 264, 1999